Phys. Status Solidi B **253,** No. 12, 2440–2445 (2016) / **DOI** 10.1002/pssb.201600326

physica status solidi b
www.pss-b.com
basic solid state physics

Optical properties of silica aerogels with embedded multiwalled carbon nanotubes

Alexander I. Chernov[*,1,2], Alexander Y. Predein[3], Alexander F. Danilyuk[3], Vladimir L. Kuznetsov[3,4], Tatyana V. Larina[3], and Elena D. Obraztsova[1,2]

[1] Prokhorov General Physics Institute, RAS, 38 Vavilov str., 119991 Moscow, Russia
[2] National Research Nuclear University MEPhI (Moscow Engineering Physics Institute), Kashirskoe hwy. 31, 115409 Moscow, Russia
[3] Boreskov Institute of Catalysis SB RAS, Lavrentieva ave. 5, 630090 Novosibirsk, Russia
[4] Novosibirsk State University, Pirogova 2, 630090 Novosibirsk, Russia

Received 20 May 2016, revised 29 June 2016, accepted 5 July 2016
Published online 25 July 2016

Keywords multiwalled carbon nanotubes, nonlinear properties, saturable absorber, silica aerogels

[*] Corresponding author: e-mail al.chernov@nsc.gpi.ru, Tel/Fax: +74995038206

Multiwalled carbon nanotubes (MWCNTs) were successfully incorporated inside silica aerogel matrix. Solid composite materials were investigated by high-resolution transmission microscopy, scanning electron microscopy, optical spectroscopy. MWCNTs in the form of small bundles and individual tubes get locked inside the aerogel between its pores resulting in the local solution-free environment for nanotubes. Optical transmission of the composite material can be modified by the amount of the added MWCNTs. Nonlinear optical properties were studied by a Z-scan technique. Composite materials demonstrate saturable absorption for femtosecond laser pulses at 515 nm wavelength that are attributed to the properties of embedded nanotubes. Silica aerogels possess significantly better thermal stability compared to polymer matrices, hosts that are frequently used for saturable absorption applications of carbon nanotubes. Solid and lightweight silica aerogels with embedded nanotubes can be used as optical elements for various photonic devices.

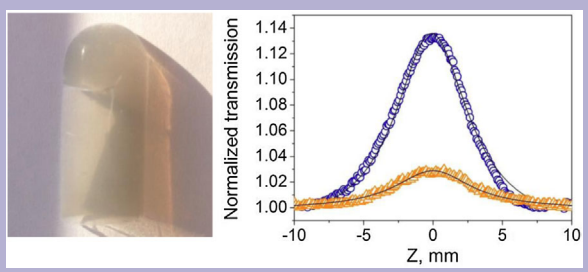

Photo of silica aerogel with embedded MWCNTs. Normalized Z-scan transmittance of silica aerogel with nanotubes for two different on-focus intensities.

1 Introduction Silica aerogels are robust, lightweight materials widely used in scientific and industrial applications due to their adjustable optical transparency, large surface area, ultrafine pore size, low dielectric constant, very low density, and high thermal stability [1]. Aerogels are applied as catalytic supports [2], absorbents of heavy metals and hypervelocity particles [3], supercapacitors [4, 5], Cherenkov detectors [6], acoustic and thermal insulators, and sensors [7]. Optical-grade aerogels are promising for photonics applications [8]. The aerogel microstructure, a 3D silica network, and its properties can be adjusted chemically by sol-gel techniques, variation of precursors, and by additional dopants. It has been demonstrated that multiwalled carbon nanotubes (MWCNTs) can serve as the reinforcing fillers to enhance the mechanical properties of the composite material [9, 10]. Inclusion of MWCNTs into aerogels influences the electrical properties [11, 12] and electrochemical characteristics [13]. An aerogel matrix can provide incorporation of MWCNTs with low bundling, so that nanotubes become partially isolated from each other in a solution-free environment. The dielectric constant in such a medium becomes similar to that of air. The local environment created around the nanotubes within aerogel makes it interesting to

investigate the optical properties of composite materials determined by embedded MWCNTs.

MWCNTs possess nonlinear optical properties. Depending on the time-scale regime of excitation nanotubes demonstrate strong optical limiting effects and saturable absorption [14]. Nonlinear properties are extensively studied in carbon materials: C_{60} [15], MWCNTs [14], single-walled carbon nanotubes [16, 17], graphene [18, 19] and, recently, in various noncarbon 2D layer materials [20, 21]. In turn, MWCNTs are considered as a material that is one of the cheapest in production and advantageous for some applications [22]. The studies of nonlinear properties mostly have been performed on liquid-phase materials. However, for applications a solid-state form is favored. Composite materials combining silica matrix and MWCNTs were reported to demonstrate nonlinear optical properties [23–25]. At the moment, carbon nanotubes embedded in polymer matrix are the most widely used as saturable absorbers for fiber lasers [26]. The transmittance of saturable absorbers increases with the input laser intensity, which can be used for mode locking and Q-switching, turning the continuous-wave laser into a pulse regime with the pulse width below 200 fs [27]. Despite the fact that such saturable absorbers are very convenient, the polymer matrix itself becomes the limiting factor, as it cannot sustain high powers when placed inside the laser resonator due to a weak thermal stability and a relatively low thermal conductivity [28]. Most of polymers used as a matrix start to deteriorate at temperatures around 200 °C [29]. We demonstrate that silica aerogels can be used as a supporting matrix instead of polymer films. They demonstrate optical transparency and no thermal degradation up to 1000 °C. Their transmission values can be changed over a wide range.

In this work, we form silica aerogels with incorporated MWCNTs, investigate the optical properties of such composite materials, demonstrate that MWCNTs embedded in silica aerogels have nonlinear saturable absorption and can be applied for lasers.

2 Experimental MWCNTs were produced via a catalytic chemical vapor deposition technique using a preformed Fe-Co catalyst at 680 °C [30]. The average MWCNT diameter is 10 nm and the average length is 0.4 μm (with variation within the range of 0.2–3 μm).

Silica aerogels were formed from tetraethoxysilane ($Si(OC_2H_5)_4$) (TEOS) in several stages. TEOS was diluted with methyl alcohol (CH_3OH). After the alcohol removal by boiling the mixture of silica-organic oligomers was diluted by ethane nitrile (C_2H_3N). This solution was used for aerogel preparation. We formed aerogels with a density of 0.25 g cm^{-3}. A typical amount of used oligomer solution was 1.9 ml and a nanotube suspension in DMF (dimethylformamide) – 1.1 ml (containing 0.01 mg of tubes per 1 ml of DMF). A liquid phase of each sample was increased up to 5 ml by DMF and water addition. Sol condensation to the gel form was promoted by NH_3. The gel was aged for 2–3 days and further acetonitrile was exchanged on isopropanol. The aerogel with embedded nanotubes was formed after the solvent removal by supercritical drying (236 °C, 5.38 MPa). MWCNTs are homogeneously dispersed in the silica aerogel matrix using DMF solutions with nanotube concentrations below 0.05 mg ml^{-1}.

The structure of silica MWCNT aerogels was characterized with transmission electron microscopy (TEM) (JEM 2010, Jeol). The samples for TEM study were deposited on copper grids without any liquid to avoid the aerogel structure destruction by capillary forces.

The Raman measurements were carried out using HeNe laser (Melles Griot) at 633 nm (1.96 eV) and ArKr ion laser (Stabilite 2018, Newport) at 514 nm (2.41 eV). The Raman spectra were recorded using LabRam HR (Horiba) and the triple monochromator spectrometer Jobin Yvon S3000 in a microconfiguration. UV-VIS-NIR optical absorption spectra were registered with a spectrophotometer Lambda-950 (Perkin Elmer).

Nonlinear optical properties were studied using the open-aperture Z-scan setup. Transmittance through the sample was measured while it was translated along the beam axis through the focus of a lens. The setup comprises the 200-fs laser pulses source emitting at 515 nm (Newport Mai Tai HP Ti:sapphire laser, 80.68 MHz repetition rate combined with Spectra-Physics Inspire Auto 100 optical parametric oscillator), linear stage (Newport IMS-500) with mounted sample, a 10-cm focal length lens, and a diode detector. The beam waist radius at the focus was estimated as 40 μm. The on-focus beam intensity was varied from 0.012 to 0.080 GW cm^{-2}. The light propagated through 3 mm of aerogel with embedded MWCNTs.

3 Results and discussion Silica aerogels with incorporated MWCNTs were prepared with an average density of 0.25 g cm^{-3}. It is a solid and nonbendable material compared to MWCNT aerogels without a silica matrix [31]. Figure 1 represents a typical image of a pristine silica aerogel and a silica aerogel with embedded nanotubes. Nanotubes are homogeneously distributed in the silica matrix. The overall inclusion of MWCNTs does not exceed 0.8 wt.% compared to the weight of the pristine aerogel. Primary SiO_2 aerogel particles of 2–7 nm form an open structure with pores of 3–20 nm (Fig. 2). TEM demonstrates

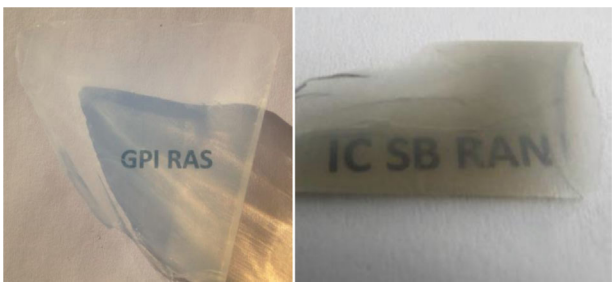

Figure 1 Left image – pristine silica aerogel, right – silica aerogel with embedded MWCNTs.

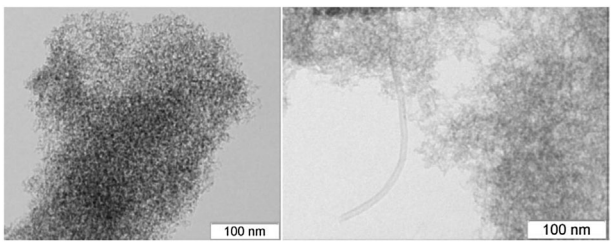

Figure 2 TEM micrographs of pristine silica aerogel (left) and aerogel with embedded MWCNTs (right).

individual nanotubes (Fig. 2 right) and some quantity of their small aggregates (2–5 nanotubes). This fact confirms that some embedded MWCNTs can be in the local environment similar to that for free-standing nanotubes in air. The silica aerogel provides the solution-free matrix. All the liquid phases get removed during the supercritical drying, and, thus, MWCNTs get trapped within the aerogel between the pores. Laser applications require materials that satisfy several requirements, e.g., thermal stability, low level of moisture absorption that may influence the optical properties, possibility to precisely control the transmission values, etc. Silica aerogels can surpass (in values of all the mentioned parameters) such composite materials as polymer matrixes with embedded nanotubes currently applied as saturable absorbers.

Figure 3 represents the optical absorption spectra of a pristine silica aerogel and an aerogel with MWCNTs. The pristine aerogels are transparent in the visible and near-infra-red spectral regions, in particular, at the telecommunication important wavelength around 1550 nm. Si–O and O–H groups contribute to the absorption at wavelengths above 2250 nm. It is important to note that formation of hydrophobic silica aerogels [32] may significantly decrease the possible influence of absorbed water on the optical

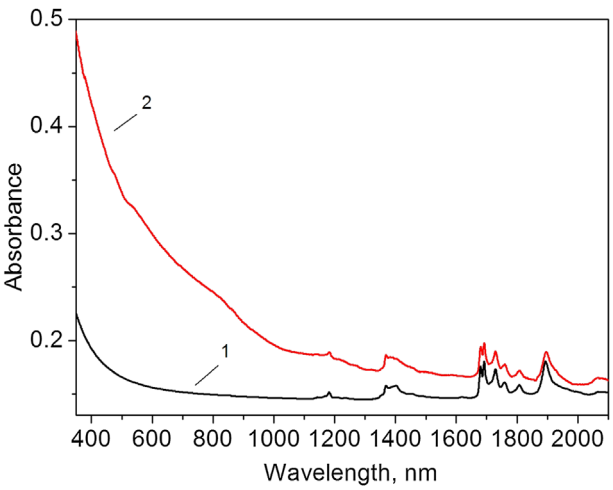

Figure 3 Optical absorption spectra of (1) – pristine silica aerogel, (2) – silica aerogel with MWCNTs. Spectrum (1) was downshifted by 0.015 with respect to the spectrum of an aerogel with embedded nanotubes for clarity.

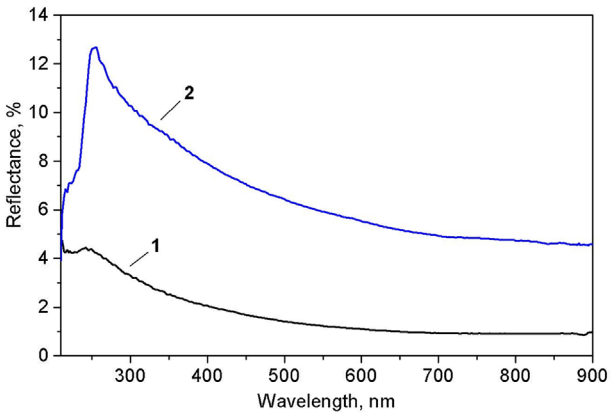

Figure 4 Diffuse reflectance spectra of pristine powder of MWCNTs (1) and a silica aerogel with embedded MWCNTs (2).

properties of composites at a wavelength of around 1900 nm. From the optical absorption spectrum of silica aerogel with MWCNTs, we estimate the transmission value of 48% at a wavelength of 515 nm. A linear extinction coefficient α_0 can be calculated from $T = \exp(-\alpha_0 L)$, where L is the optical path through the sample. The transmission can be controlled by the amount of nanotubes introduced into the aerogel during formation for fitting the requirements for the exact application. Diffuse reflectance spectra (DRS, Fig. 4) and Raman spectra (Fig. 5) of silica aerogels with MWCNTs demonstrate the inclusion of MWCNTs inside the silica aerogels. These spectra have all the spectroscopic features typical of MWCNTs with some deviation from the spectra of pristine nanotubes. Thus, the comparison of DRS demonstrates the more intensive reflectance, which may be explained by isolation of individual nanotubes in the aerogel matrix, while in powders nanotubes have numerical contacts causing high conductivity and lower optical reflectance [33].

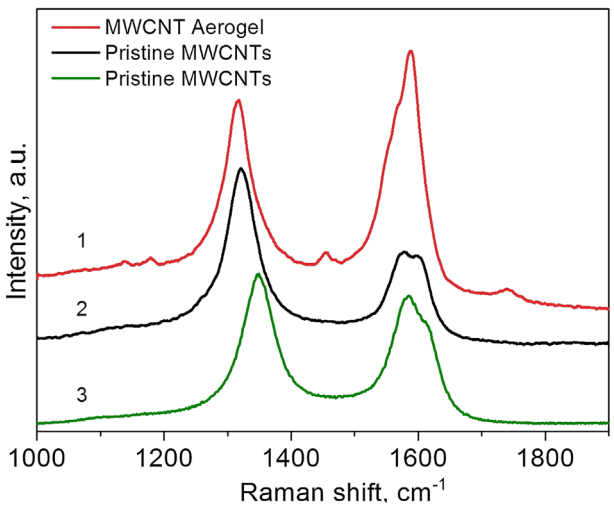

Figure 5 Raman spectra of (1) – MWCNT–aerogel composite, (2) – pristine MWCNTs. Both spectra measured with 633 nm excitation wavelength. (3) – Raman spectrum of pristine MWCNTs measured with 514-nm excitation wavelength.

At the same time, the elimination of precipitated agglomerates during the preparation of nanotube suspensions before aerogel production resulted in the increase of the Raman G-band (1500–1650 cm^{-1}) to the D-band (1250–1400 cm^{-1}) intensity ratio in aerogels compared to pristine MWCNTs. A disorder-induced D-band demonstrates the dispersion behavior [34] (Fig. 5). Regardless of the testing point within the sample, the Raman spectra of MWCNTs are similar with the equal ratio between the G- and D-band intensities and the same peak positions confirming a homogeneous distribution of nanotubes within the aerogel.

Nonlinear optical properties were studied by the open-aperture Z-scan technique. An excitation was performed with the fs laser pulses at 515 nm (2.4 eV). Moving the sample along the laser beam through the focus of the lens we detect the increase of transmittance, indicating the saturable absorption response of the sample (Fig. 6).

The measurements were performed multiple times within the same position in the aerogel and were reproducible, proving that the effect is not due to the burning of nanotubes. The on-focus beam intensity used for the studies did not exceed 0.08 GW cm^{-2}. Previously, it has been reported that laser excitation may significantly affect carbon nanotubes [35]. Laser-induced change of optical properties of carbon-based materials [36–39] can result, for instance, in the effect of transparency increase. Such effects were explained by the chemical reaction with the solvent that was used for suspending carbon materials. The nonlinear properties of MWCNTs composites produced by sol-gel technique have been reported [23–25]. The authors of the works [23, 25] discussed the optical limiting properties of such materials. We note that embedded MWCNTs are in the solution-free environment that cannot influence the nonlinear optical properties. A pristine aerogel itself showed no changes in transmittance during Z-scans, validating that the saturable absorption is determined by the

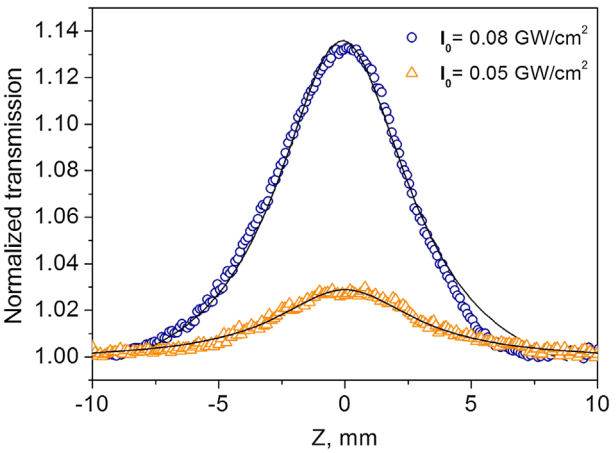

Figure 6 Normalized Z-scan transmittance of silica aerogel with embedded MWCNTs for two different on-focus intensities. Solid lines are the theoretical fit curves.

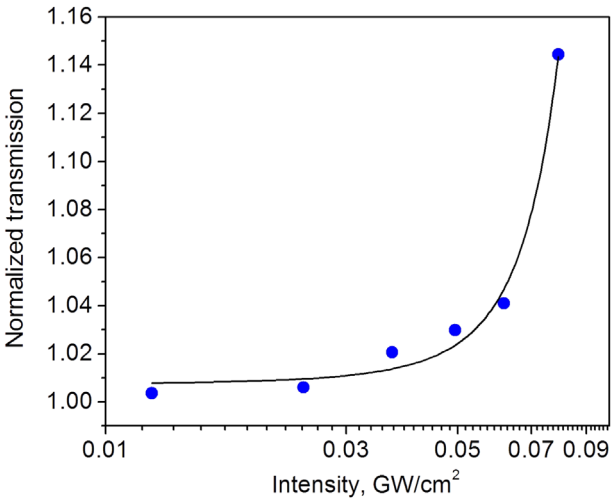

Figure 7 Normalized transmission as a function of the input fluence.

MWCNTs. We clearly detect the dependence between the normalized transmission and incident laser intensity in the focal point (Fig. 7).

In order to estimate the nonlinear coefficient β_{eff} we address the nonlinear optical theory and Z-scan formalism [40]. The total absorption α consists of linear and nonlinear parts $\alpha(I) = \alpha_0 + \beta_{eff} I$. A normalized transmission can be defined by the following expression:

$$T(z) = 1 - \frac{I_0 L_{eff} \beta}{\sqrt{8}\left(1 + \left(\frac{z}{z_0}\right)^2\right)}, \quad (1)$$

where I_0 is the laser beam intensity at the focus ($z = 0$), L_{eff} is the effective thickness, $L_{eff} = (1 - \exp(-\alpha_0 L))/\alpha_0$, L is the thickness of the sample, $z_0 = \pi\omega_0^2\lambda$ is the diffraction length of the beam, ω_0 is the beam waist radius, and λ is the laser wavelength. Performing the fitting (Fig. 6) by using Eq. (1), we determine the value of $\beta_{eff} = -28 \pm 3$ cm GW^{-1}, cf. Table 1.

Starting with on-focus laser beam intensities above 0.03 GW cm^{-2}, we detect the transmission increase around the focal point. The most pronounced effect was obtained in the samples with homogeneously dispersed MWCNTs within the silica aerogel. It is important to note that scattering in such samples can be modified by chemical processing of the sol-gel technique, additionally during the MWCNT introduction depending on the solvent and also by polishing of the final solid material. A saturable absorption

Table 1 Linear and nonlinear coefficients for silica aerogel with embedded MWCNTs.

T (%)	α_0 (cm^{-1})	$\lvert\beta_{eff}\rvert$ (cm/GW)
48	2.45	28 ± 3

for the fs laser pulses of aerogels with embedded MWCNTs confirms the possibility of application of such composite materials as ultrafast nonlinear optical elements. The thermal stability over a wide temperature range, a possibility to control the transmission, and an extraordinary environment that can be established for trapped nanotubes inside the silica aerogel may be considered as additional advantages. The locked small bundles of tubes and in some cases even individual nanotubes, noninteracting with other tubes, are the main explanation for strong nonlinear optical properties of the silica aerogel–nanotube composite material.

4 Conclusions In this work, we demonstrate the fabrication of silica aerogels with embedded MWCNTs. Nanotubes in such composite materials are homogeneously distributed within the aerogel matrix. With that, we identify small bundles and individual nanotubes locked in the silica aerogel porous matrix. A solvent-free local environment decreases the interaction between the nanotubes. The pristine silica aerogels are transparent over a wide spectral range, making this type of matrix suitable for many photonic applications. The optical properties of composite materials are dominantly influenced by MWCNTs. For instance, the transmission value can be controlled by the amount of introduced nanotubes. The nonlinear optical properties were studied by the open-aperture Z-scan technique. Silica aerogel–MWCNT composites demonstrate a saturable absorption for 200-fs laser pulses at a 515-nm wavelength. The nonlinear properties are attributed to the incorporated MWCNTs.

Silica aerogels can be used as a matrix supporting nanotubes for various photonic devices, e.g., such as saturable absorbers for mode locking. Silica aerogels demonstrate significantly better thermal stability compared to polymer matrices that are frequently used for saturable absorption applications, but suffer from thermal degradation at temperatures already above 200 °C. Silica aerogels are capable of significantly enhancing the laser power limits, while retaining the best properties of nanotubes.

Acknowledgements The work was supported by RFBR projects: 14-02-00777, 15-32-70005 mol_a_mos, 15-59-31817 RT-omi, 16-32-50122, partially by FASO (project V.45.3.5) and by the Competitiveness Program of NRNU MEPhI. We thank Prof. V. I. Belotelov in the Russian Quantum Center for the use of his group's facilities for nonlinear optics studies and A. V. Ischenko for TEM studies.

References

[1] J. Fricke and T. Tillotson, Thin Solid Films **297**, 212 (1997).
[2] M. L. Anderson, R. M. Stroud, and D. R. Rolison, Nano Lett. **2**, 235 (2002).
[3] P. Tsou, J. Non-Cryst. Solids **186**, 415 (1995).
[4] G. Oskam and P. C. Searson, J. Phys. Chem. B **102**, 2464 (1998).
[5] X. Du, C. Wang, T. Li, and M. Chen, Ionics **15**, 561 (2009).
[6] M. Yu. Barnyakov, V. S. Bobrovnikov, A. R. Buzykaev, A. F. Danilyuk, S. F. Ganzhur, I. I. Goldberg, G. M. Kolachev, S. A. Kononov, E. A. Kravchenko, G. D. Minakov, A. P. Onuchin, G. A. Savinov, and V. A. Tayursky, Nucl. Instrum. Methods Phys. Res. A **453**, 326 (2000).
[7] N. Leventis, I. A. Elder, D. R. Rolison, M. L. Anderson, and C. I. Merzbacher, Chem. Mater. **11**, 2837 (1999).
[8] J. G. Duque, C. E. Hamilton, G. Gupta, S. A. Crooker, J. J. Crochet, A. Mohite, H. Htoon, K. A. DeFriend Obrey, A. M. Dattelbaum, and S. K. Doorn, ACS Nano **5**, 6686 (2011).
[9] Y. Zhang, Y. Shen, D. Han, Z. Wang, J. Song, and L. Niu, J. Mater. Chem. **16**, 4592 (2006).
[10] I.-K. Jung, J. L. Gurav, U. K. H. Bangi, S. Baek, and H.-H. Park, J. Non-Cryst. Solids **358**, 550 (2012).
[11] X. Changshu, P. Yubai, L. Xuejian, S. Xiaomei, S. Xingwei, and J. Guo, J. Nanosci. Nanotechnol. **6**, 3835 (2006).
[12] C. Xiang, Y. Pan, X. Liu, X. Sun, X. Shi, and J. Guo, Appl. Phys. Lett. **87**, 123103 (2005).
[13] V. G. Gavalas, R. Andrews, D. Bhattacharyya, and L. G. Bachas, Nano Lett. **1**, 719 (2001).
[14] H. I. Elim, W. Ji, G. H. Ma, K. Y. Lim, C. H. Sow, and C. H. A. Huan, Appl. Phys. Lett. **85**, 1799 (2004).
[15] R. A. Ganeev, A. I. Ryasnyansky, V. I. Redkorechev, K. Fostiropoulos, G. Priebe, and T. Usmanov, Opt. Commun. **225**, 131 (2003).
[16] A. Maeda, S. Matsumoto, H. Kishida, T. Takenobu, Y. Iwasa, M. Shiraishi, M. Ata, and H. Okamoto, Phys. Rev. Lett. **94**, 047404 (2005).
[17] A. V. Tausenev, E. D. Obraztsova, A. S. Lobach, V. I. Konov, A. V. Konyashchenko, P. G. Kryukov, and E. M. Dianov, Quantum Electron. **37**, 847 (2007).
[18] J. Wang, Y. Hernandez, M. Lotya, J. N. Coleman, and W. J. Blau, Adv. Mater. **21**, 2430 (2009).
[19] V. R. Sorochenko, E. D. Obraztsova, P. S. Rusakov, and M. G. Rybin, Quantum Electron. **42**, 907 (2012).
[20] K. Wang, J. Wang, J. Fan, M. Lotya, A. O'Neill, D. Fox, Y. Feng, X. Zhang, B. Jiang, Q. Zhao, H. Zhang, J. N. Coleman, L. Zhang, and W. J. Blau, ACS Nano **7**, 9260 (2013).
[21] Z. Luo, D. Wu, B. Xu, H. Xu, Z. Cai, J. Peng, J. Weng, S. Xu, C. Zhu, F. Wang, Z. Sun, and H. Zhang, Nanoscale **8**, 1066 (2016).
[22] Y. Zhu, H. I. Elim, Y.-L. Foo, T. Yu, Y. Liu, W. Ji, J.-Y. Lee, Z. Shen, A. T. S. Wee, J. T. L. Thong, and C. H. Sow, Adv. Mater. **18**, 587 (2006).
[23] C. Zheng, M. Feng, Y. Du, and H. Zhan, Carbon **47**, 2889 (2009).
[24] M. Pokrass, Z. Burshtein, R. Gvishi, and M. Nathan, Opt. Mater. Express **2**, 825 (2012).
[25] Z. Hongbing, C. Wenzhe, W. Minquan, Zhengchan, and Z. Chunlin, Chem. Phys. Lett. **382**, 313 (2003).
[26] T. Hasan, Z. Sun, F. Wang, F. Bonaccorso, P. H. Tan, A. G. Rozhin, and A. C. Ferrari, Adv. Mater. **21**, 3874 (2009).
[27] A. V. Tausenev, E. D. Obraztsova, A. S. Lobach, A. I. Chernov, V. I. Konov, P. G. Kryukov, A. V. Konyashchenko, and E. M. Dianov, Appl. Phys. Lett. **92**, 171113 (2008).
[28] X. Huang, P. Jiang, and T. Tanaka, IEEE Electr. Insul. Mag. **27**, 8 (2011).
[29] N. A. El-Zaher and W. G. Osiris, J. Appl. Polym. Sci. **96**, 1914 (2005).
[30] D. V. Krasnikov, A. N. Shmakov, V. L. Kuznetsov, K. V. Elumeeva, and A. V. Ishchenko, Bull. Russ. Acad. Sci.: Phys. **77**, 155 (2013).

[31] J. Zou, J. Liu, A. S. Karakoti, A. Kumar, D. Joung, Q. Li, S. I. Khondaker, S. Seal, and L. Zhai, ACS Nano **4**, 7293 (2010).
[32] A. P. Rao, A. V. Rao, and G. M. Pajonk, Appl. Surf. Sci. **253**, 6032 (2007).
[33] V. L. Kuznetsov, S. I. Moseenkov, K. V. Elumeeva, T. V. Larina, V. F. Anufrienko, A. I. Romanenko, O. B. Anikeeva, and E. N. Tkachev, Phys. Status Solidi B **248**, 2572 (2011).
[34] J. Kürti, V. Zólyomi, A. Grüneis, and H. Kuzmany, Phys. Rev. B **65**, 165433 (2002).
[35] E. D. Obraztsova, S. N. Bokova, V. L. Kuznetsov, A. N. Usoltseva, V. I. Zaikovskii, U. Dettlaff-Weglikowska, S. Roth, and H. Kuzmany, AIP Conf. Proc. **685**, 215 (2003).
[36] M. M. Gen, V. L. Kuznetsov, D. L. Bulatov, T. N. Mogileva, S. I. Moseenkov, and A. V. Ishchenko, Quantum Electron. **39**, 342 (2009).
[37] G. M. Mikheev, V. L. Kuznetsov, D. L. Bulatov, T. N. Mogileva, S. I. Moseenkov, and A. V. Ishchenko, Tech. Phys. Lett. **35**, 162 (2009).
[38] G. M. Mikheev, V. L. Kuznetsov, K. G. Mikheev, T. N. Mogileva, and S. I. Moseenkov, Tech. Phys. Lett. **37**, 831 (2011).
[39] G. M. Mikheev, V. L. Kuznetsov, K. G. Mikheev, T. N. Mogileva, M. A. Shuvaeva, and S. I. Moseenkov, Tech. Phys. Lett. **39**, 337 (2013).
[40] M. Sheik-Bahae, A. A. Said, T. H. Wei, D. J. Hagan, and E. W. V. Stryland, IEEE J. Quantum Electron. **26**, 760 (1990).